MOLECULAR AND CELLULAR BIOLOGY, Nov. 1997, p. 6517–6525 Vol. 17, No. 11
0270-7306/97/$04.00+0

Coordination of the Mating and Cell Integrity Mitogen-Activated Protein Kinase Pathways in *Saccharomyces cerevisiae*

BENJAMIN M. BUEHRER AND BEVERLY ERREDE*

Department of Biochemistry and Biophysics, University of North Carolina at Chapel Hill, Chapel Hill, North Carolina 27599-7260

Received 12 June 1997/Returned for modification 22 July 1997/Accepted 31 July 1997

Mating pheromone stimulates a mitogen-activated protein (MAP) kinase activation pathway in *Saccharomyces cerevisiae* that induces cells to differentiate and form projections oriented toward the gradient of pheromone secreted by a mating partner. The polarized growth of mating projections involves new cell wall synthesis, a process that relies on activation of the cell integrity MAP kinase, Mpk1. In this report, we show that Mpk1 activation during pheromone induction requires the transcriptional output of the mating pathway and protein synthesis. Consequently, Mpk1 activation occurs subsequent to the activation of the mating pathway MAP kinase cascade. Additionally, Spa2 and Bni1, a formin family member, are two coil-coil-related proteins that are involved in the timing and other aspects of mating projection formation. Both proteins also affect the timing and extent of Mpk1 activation. This correlation suggests that projection formation comprises part of the pheromone-induced signal that coordinates Mpk1 activation with mating differentiation. Stimulation of Mpk1 activity occurs through the cell integrity phosphorylation cascade and depends on Pkc1 and the redundant MAP/Erk kinases (MEKs), Mkk1 and Mkk2. Surprisingly, Mpk1 activation by pheromone was only partially impaired in cells lacking the MEK kinase Bck1. This Bck1-independent mechanism reveals the existence of an alternative activator of Mkk1/Mkk2 in some strain backgrounds that at least functions under pheromone-induced conditions.

In the budding yeast *Saccharomyces cerevisiae*, separate mitogen-activated protein kinase (MAPK) cascades control responses to mating pheromone, high osmolarity, nutrient starvation, and physical distortions associated with polarized growth and heat shock (19, 31). The components of different cascades do not compensate for one another, and each cascade functions in such a way that a given stimulus activates only the appropriate cellular response. However, certain cellular responses require the output of more than one cascade. For example, the mating and cell integrity pathways each have a role in the differentiation of vegetative cells into a mating-competent form. Among other responses, the mating pathway stimulates the formation of projections oriented toward the gradient of mating pheromone secreted by a mating partner (43). The cell integrity pathway, which controls cell wall synthesis, was found to be necessary for cell viability during projection formation (9, 30, 37). The participation of this second pathway in pheromone response makes sense because new cell wall synthesis is needed during polarized growth associated with mating projection formation. Yet how their activities are coordinated for this morphogenetic process remains unknown.

The major components of the mating pathway and their roles in pheromone-induced signal transmission are well defined (6, 19, 31). The mating pheromone from one mating type binds to the cell surface receptor on the opposite mating type (Ste2 and Ste3). This cell surface interaction triggers the activation of a heterotrimeric G protein (Gα-Gpa1, Gβ-Ste4, and Gγ-Ste18), a Rho-family GTPase (Cdc42) and its exchange factor (Cdc24), and the protein kinase, Ste20. By an as yet undefined mechanism, the signal from the Gβγ dimer also activates a MAPK cascade comprised of Ste11 (a MEK kinase [MEKK]), Ste7 (a MAPK/ERK kinase [MEK]), and Fus3 and Kss1 (MAPKs; also called ERKs). Ste5 promotes interactions between components of this cascade and isolates them from spurious interactions with counterparts from other cascades (3, 34, 39, 49). Fus3 and Kss1 have partially redundant functions. Activation of either enzyme is sufficient for the pheromone-induced and Ste12-dependent transcriptional activation of mating-specific genes. Fus3 has an additional role in promoting the Far1-dependent cell cycle arrest at G_1 (8).

The cell integrity MAPK cascade is comprised of Bck1 (a MEKK), Mkk1 and Mkk2 (MEKs), and Mpk1 (a MAPK). This cascade is stimulated by heat shock and polarized growth associated with proliferation and pheromone induction (9, 22, 51). The yeast homolog of protein kinase C, Pkc1, functions upstream of this cascade and is activated by a small GTPase of the Rho family, Rho1 (23, 32). Disruption of Pkc1 or any of the genes whose products function downstream of Pkc1 results in an osmotic remedial lytic phenotype due to a failure in proper cell wall construction (30, 37). Notably, *pkc1* mutants exhibit a nonconditional lytic phenotype whereas mutants containing disruptions in the MAPK cascade exhibit a lytic phenotype only at elevated temperature. The more severe phenotype of *pkc1* mutants has led to the proposal that the pathway bifurcates just below Pkc1, with Bck1 heading the MAPK cascade branch. The other postulated arm of the pathway remains ill defined (27, 29).

To learn how the pheromone-induced signal intersects the cell integrity pathway, we studied cells deficient in components of the mating and cell integrity pathways. The analyses suggest that Mpk1 activation occurs as a consequence of pheromone-induced events rather than by a more direct mechanism. This activation is strictly dependent on Pkc1 and Mkk1/Mkk2 but surprisingly is only partially dependent on Bck1. Thus, at least in some strain backgrounds, transmission of the pheromone-dependent signal has available another component that functions at the level of Bck1. We further discovered that Spa2 and

* Corresponding author. Mailing address: Department of Biochemistry and Biophysics, CB#7260, University of North Carolina, Chapel Hill, NC 27599-7260. Phone: (919) 966 3628. Fax: (919) 966 4812. E-mail: errede@nun.oit.unc.edu.

TABLE 1. *S. cerevisiae* strains used

Strain[a]	Relevant genotype	Reference or source
D13au	*MAT***a** *ade1 his2 leu2-3,112 trp1-1a ura3ΔNS cdc28-13*	35
BB106	*MAT***a** *ade1 his2 leu2-3,112 trp1-1a ura3ΔNS cdc28-13 ste12Δ::LEU2*	This study
BB108	*MAT***a** *ade1 his2 leu2-3,112 trp1-1a ura3ΔNS cdc28-13 bck1Δ::URA3*	This study
BB113	*MAT***a** *ade1 his2 leu2-3,112 trp1-1a ura3ΔNS cdc28-13 spa2Δ::TRP1*	This study
BB121	*MAT***a** *ade1 his2 leu2-3,112 trp1-1a ura3ΔNS cdc28-13 mkk1Δ::LEU2 mkk2Δ::URA3*	This study
BB126	*MAT***a** *ade1 his2 leu2-3,112 trp1-1a ura3ΔNS cdc28-13 bni1Δ::URA3*	This study
BB127	*MAT***a** *ade1 his2 leu2-3,112 trp1-1a ura3ΔNS cdc28-13 spa2Δ::TRP1 bni1Δ::URA3*	This study
BB131	*MAT***a** *ade1 his2 leu2-3,112 trp1-1a ura3ΔNS cdc28-13 ste4Δ::URA3*	This study
TME-3/28	*MAT***a** *ade1 his2 leu2-3,112 trp1-1a ura3ΔNS cdc28-4* (*pkc1*^{ts})	35

[a] All strains are isogenic to BF264-15D (41).

Bni1, two proteins involved in the timing and other aspects of mating projection formation, affect the timing and extent of Mpk1 activation (2, 16, 33). This correlation suggests that projection formation comprises part of the signal that leads to Mpk1 activation during pheromone-induced mating differentiation.

MATERIALS AND METHODS

Yeast strains, media, and genetic manipulations. The yeast strains used in this study are all derived from BF264-15D and are listed in Table 1 (41). Unless otherwise specified, standard media and genetic procedures were used (44). Yeast cells were transformed by the method of Ito et al. (21). Construction of yeast strains containing deletions in either the pheromone pathway or the cell integrity pathway was carried out by the gene replacement method of Rothstein (42). Plasmids pSUL16 (*ste12Δ::LEU2*) (from S. Fields [13]), pL280 (*bck1Δ::URA3*) (from D. Levin [29]), p211 (*spa2Δ2::TRP1*) (from M. Snyder [16]), pBluescript[*mkk1Δ::LEU2*] (from K. Irie [20]), pBluescript[*mkk2Δ::URA3*] (from K. Irie [20]), and pB6Δ (*bni1Δ::URA3*) (from J. Pringle) were the sources of alleles for gene replacements (Table 1).

Plasmid YEp352[*MPK1-HA*; *URA3*] (from D. Levin [22]) expresses Mpk1^{HA}, which is Mpk1 with an in-frame fusion to three tandem repeats of an epitope from the influenza virus hemagglutinin protein (HA) on a 2μm plasmid (48). The 2μm plasmids pNC458 and pNC507 were constructed to change the selectable marker of overexpressed Mpk1^{HA} by inserting an *Eco*RI-*Sph*I fragment of YEp352[*MPK1-HA*] containing the Mpk1^{HA} fusion and inserting it into 2μm YEplac112 (*TRP1*) and pRS425 (*LEU2*) vectors, respectively (4, 17). These plasmids were transformed into the appropriate yeast cells to monitor Mpk1 activity by an immune complex kinase assay.

Culture conditions and preparation of protein extracts. Cells were grown to a density of ~10^7 cells/ml at room temperature (23°C) in appropriate media prior to a 1:1 dilution with prewarmed media (~55°C). Cultures were then incubated at 37°C for 1.5 to 2 h until the cells, which have a temperature-sensitive *cdc28* allele, accumulated at the G_1 block as large unbudded cells. At this time ($t = 0$), a 50-ml sample of each culture was removed for preparation of protein extracts and mating pheromone was added to the remaining cultures (50 nM α-factor). Samples (50 ml) were removed at the indicated times following pheromone addition, and protein extracts were prepared.

Yeast cells were harvested by centrifugation, and cell pellets were washed once with 1 ml of ice-cold stop buffer (50 mM Tris [pH 7.5], 150 mM NaCl, 5 mM EDTA, 0.1% Nonidet P-40, 15 mM *p*-nitrophenyl phosphate, 15 mM sodium pyrophosphate, 10 mM NaF, 0.5 mM Na_3VO_4, and 1 mM phenylmethylsulfonyl fluoride). The pellet was suspended in 0.4 ml of stop buffer containing additional protease inhibitors (40 μg of aprotinin and 20 μg of leupeptin per ml). Cells were broken by vigorous shaking with glass beads on an IKA platform mixer at 4°C for a total of 10 min. Glass beads and cellular debris were removed by centrifugation at 4°C, and the supernatant was transferred to a new tube. An equal volume of saturated ammonium sulfate solution was added, and the mixture was incubated at 4°C for 30 min with mild agitation. Precipitated protein was collected by centrifugation for 10 min at 4°C, and the supernatant was removed by aspiration. The resulting protein pellet was suspended in storage buffer containing 25 mM HEPES (pH 8.0), 5 mM EDTA, 150 mM NaCl, 1.0% Nonidet P-40, 20% glycerol, 15 mM 1,4-dinitrophenyl phosphate, 0.1 mM Na_3VO_4, 40 μg of aprotinin per ml, 20 μg of leupeptin per ml, and 1 mM phenylmethylsulfonyl fluoride and flash frozen in liquid nitrogen for storage at −80°C until needed.

Immunoprecipitation and in vitro kinase assay. Immunoprecipitations and kinase assays were performed by the method of Kamada et al. (22). Briefly, 200-μg aliquots of protein extracts were incubated with 3.2 μg of anti-HA monoclonal antibody (clone 12CA5; Boehringer Mannheim) at 4°C for 60 min, and 20 μl of packed prewashed protein A-Sepharose (Pharmacia-LKB) beads was incubated with the antibody-protein complex at 4°C for 60 min. The beads were extensively washed and placed in kinase buffer (25 mM HEPES [pH 7.5], 15 mM $MgCl_2$, 5 mM EGTA, 1 mM dithiothreitol, 0.1 mM Na_3VO_4, 15 mM 1,4-dinitrophenyl phosphate, 20 μg of leupeptin per ml, 40 μg of aprotinin per ml) containing 5 μg of myelin basic protein (MBP; from bovine brain; Sigma) as the substrate. Kinase reactions were initiated by the addition of 2.2 μl of an ATP mixture (2.0 μl of 1 mM ATP, 0.2 μl of [γ-^{32}P]ATP [DuPont-NEN]) and allowed to proceed for 30 min at 30°C before termination by addition of 20 μl of 2× sodium dodecyl sulfate-polyacrylamide gel electrophoresis (SDS-PAGE) sample buffer and boiling for 5 min. The resulting mixture was fractionated by SDS-PAGE (25), and incorporation of ^{32}P into the protein substrate was determined by PhosphorImager (Molecular Dynamics) analysis of the dried gels.

Protein extracts from strains expressing Mpk1 were analyzed by Western blotting to verify that comparable amounts of Mpk1 were produced in all genetic backgrounds analyzed. The amount of anti-HA antibody and protein A-Sepharose beads used to immunoprecipitate Mpk1 was experimentally determined to satisfy two conditions: first, the level of Mpk1 in the protein extracts was not limiting; second, the amount of Mpk1 immunoprecipitated was still in the linear range of the assay. In developing the standard assay conditions, immunoblot analysis of the immunoprecipitation kinase assay samples was performed to verify that equal amounts of Mpk1 were routinely present in immune complexes. Once reproducibility was established, visual inspection of the Coomassie blue-stained gels (immunoglobulin G) was used to verify even loading of samples and, by inference, equal amounts of Mpk1.

Immunoblot analysis. Protein samples (100 μg) were fractionated by SDS-PAGE using 7.5% polyacrylamide gels and transferred to nitrocellulose membranes (Schleicher & Schuell), using a semidry transfer apparatus (LKB). Antiphosphotyrosine antibodies (Upstate Biotechnology, Inc.) were used (1 μg/ml) as the primary antibody to probe the membrane. Secondary antibodies of anti-mouse immunoglobulin G conjugated to horseradish peroxidase were used with the ECL detection system as described by the vendor (Amersham).

RESULTS

Mating pheromone stimulates Mpk1 activity. To determine how Mpk1 is specifically activated by mating pheromone, we used a strain with a genetic background that enabled us to separate the pheromone-induced activation from that caused by proliferation. This strain (13Dau) carries a *cdc28-13* temperature-sensitive mutation that causes cells to stop proliferating and arrest in the G_1 phase of the cell cycle at the nonpermissive temperature (37°C) (35, 41). Fortuitously, neither the *cdc28-13* strain (13Dau) nor its *CDC28* parent (BF264-15D) activated the Pkc1 pathway in response to heat shock (data not shown). This circumstance eliminates any contributions to Mpk1 activation from the temperature shift used to block proliferation (22). Yeast cultures expressing Mpk1^{HA} from a 2μm plasmid were arrested in G_1 at 37°C prior to the addition of pheromone and maintained at 37°C for the duration of the experiment. Protein extracts were prepared from cells immediately before addition of pheromone ($t = 0$) and at indicated times after the addition. Mpk1 catalytic competence requires phosphorylation of a tyrosine and a threonine residue located within the so-called activation loop. Therefore, Mpk1 activity was monitored by following changes in its phosphotyrosine content on Western blots and by measuring its kinase activity in immune complex assays using MBP as the substrate.

Consistent with previous studies using either a *CDC28* or a *cln1 cln2 GAL-cln3* strain (on glucose), the experiment with

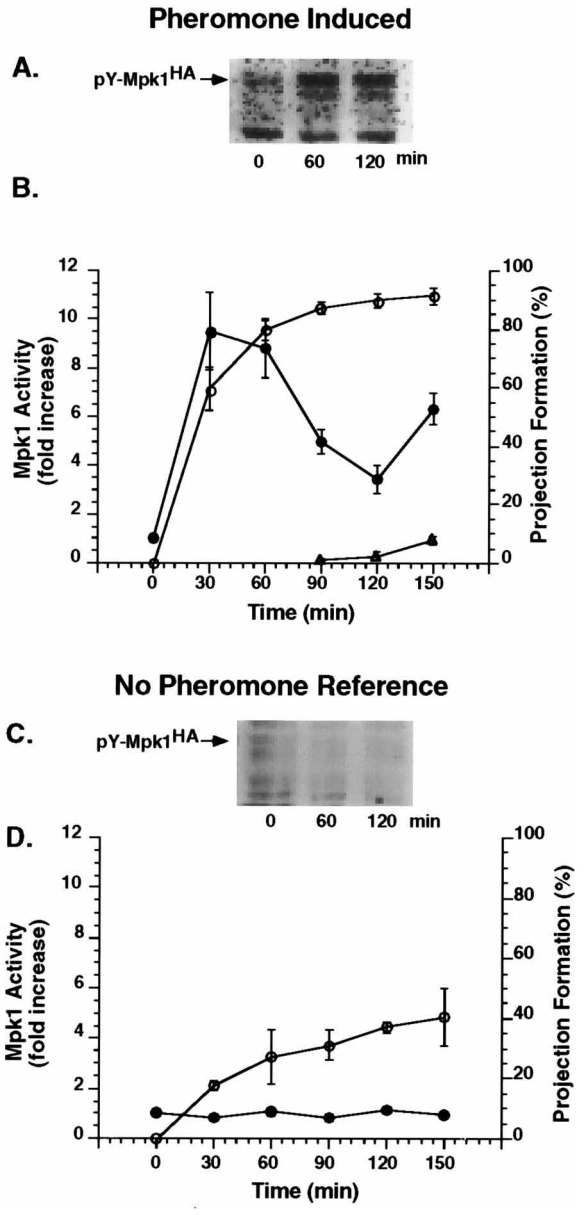

FIG. 1. Pheromone-induced activation of Mpk1. Cultures of a *cdc28-13* strain (13Dau) were arrested in G_1 at 37°C. Results are from these arrested cultures either induced with mating pheromone (50 nM α-factor, $t = 0$) (A and B) or maintained as a reference without pheromone (C and D). (A and C) Western blots showing tyrosine-phosphorylated Mpk1 ($pY\text{-}Mpk1^{HA}$) at indicated times. (B and D) Mpk1 activity in immune complex kinase assays and projection formation of cells in culture. Values (closed circles) are the amount of ^{32}P-MBP quantified by PhosphorImager analysis at each time relative to that at $t = 0$. Right axis, projection formation. The percentages of cells with one (open circles) or two (triangles) mating projections are calculated from microscopic examination of at least 100 cells from the culture at each time point. Data shown in panels B and D are averages of seven and two experiments, respectively. Bars show the deviation in the measurements. Panels A and C are representative examples of the trials.

cdc28-13 arrested cells showed a marked increase in tyrosine-phosphorylated Mpk1(pY-Mpk1) and in Mpk1 activity upon pheromone induction (Fig. 1) (9, 51). Quantification of ^{32}P-phosphorylated MBP from SDS-PAGE-fractionated immune complex kinase assays revealed two phases of increased Mpk1 activity (Fig. 1B). One peak occurred at 60 min after pheromone addition, and the other occurred after 120 min. Notably, the first and second rises in activity paralleled the increase in the appearance of first and second mating projections, respectively, on cells in the culture (Fig. 1B and 2A). By contrast, there was no increase in Mpk1 activity over the time course of the experiment for the no-pheromone reference culture (Fig. 1D).

Signal transduction through the mating pathway is required for pheromone-induced Mpk1 activation. The pheromone-induced signal for the mating pathway is transduced by the Gβγ dimer of the receptor-coupled G protein. To learn if Gβγ also transduces the pheromone-dependent signal leading to activation of Mpk1, we analyzed Mpk1 activation in a *cdc28-13 ste4*Δ strain (BB131) that lacks the Gβ-Ste4 subunit. These cells did not form projections, accumulate tyrosine-phosphorylated Mpk1(pY-Mpk1), or show an increase in Mpk1 kinase activity (Fig. 3A and B). Thus, Gβγ is required for pheromone induction of Mpk1 activity.

To determine whether the output of the mating pathway cascade was required for Mpk1 activation, a *cdc28-13 ste12*Δ strain (BB106) that lacks the Ste12 transcription factor was analyzed as before. Normally, *ste12* mutant strains do not arrest in G_1 or form mating projections but continue to proliferate by budding (18). However, at the nonpermissive temperature in the *cdc28-13* strain background, the condition of G_1 arrest is met independently of the output of the mating pathway. Consequently, in response to pheromone, *cdc28-13 ste12*Δ cells formed mating projections, albeit to a lesser extent than *cdc28-13 STE12* cells (Fig. 2B and 3D). However, there was no increase in Mpk1 activity even though there was an increase in pY-Mpk1 (Fig. 3C and D). Because MAPK family members have a propensity to autophosphorylate on the tyrosine but not threonine of the activation loop, the inactive species that accumulates under these conditions could be the monoautophosphorylated enzyme (1, 10). Regardless of the origin or site of tyrosine phosphorylation, the disparity between the phosphotyrosine and kinase assays underscores the risk in using tyrosine phosphorylation as the sole criterion for Mpk1 activity. Nevertheless, the failure of pheromone to increase Mpk1 activity in *ste12*Δ cells shows that the entire mating pathway is required for propagation of the signal leading to Mpk1 activation.

It was shown previously that Ste12 is not required for activation of the mating pathway kinase cascade by monitoring FUS3/KSS1-dependent hyperphosphorylation of Ste7 induced by pheromone. However, the finding was documented in a different strain background and under different experimental conditions (52). To confirm that function of the MAPK cascade is not impeded in the *ste12*Δ strain studied here, Fus3 kinase activity was determined by an immune complex kinase assay using extracts from the BF264-15D strain background. Under the conditions of our temperature shift and arrest protocol, Fus3 activity was induced ~4-fold in both *ste12*Δ and *STE12* strains by 5 min after pheromone stimulation (data not shown). This result and the finding that G_1-arrested *ste12*Δ cells still formed mating projections shows that a deficiency of Ste12 did not cause a failure of these cells to sense pheromone. Nevertheless, *ste12* cells express fivefold less pheromone receptor (Ste2) than wild-type cells (12). Therefore, it is possible that there is less signal in *ste12*Δ cells than in wild-type cells and that the signal threshold for Fus3 activation and projection formation is lower than for Mpk1 activation. Alternatively, the activation of Mpk1 might specifically require the synthesis of a Ste12-dependent gene product.

To test the latter possibility, a culture of the *cdc28-13 STE12* strain (13Dau) was arrested in G_1 at the nonpermissive temperature and then treated with 50 μg of cycloheximide per ml

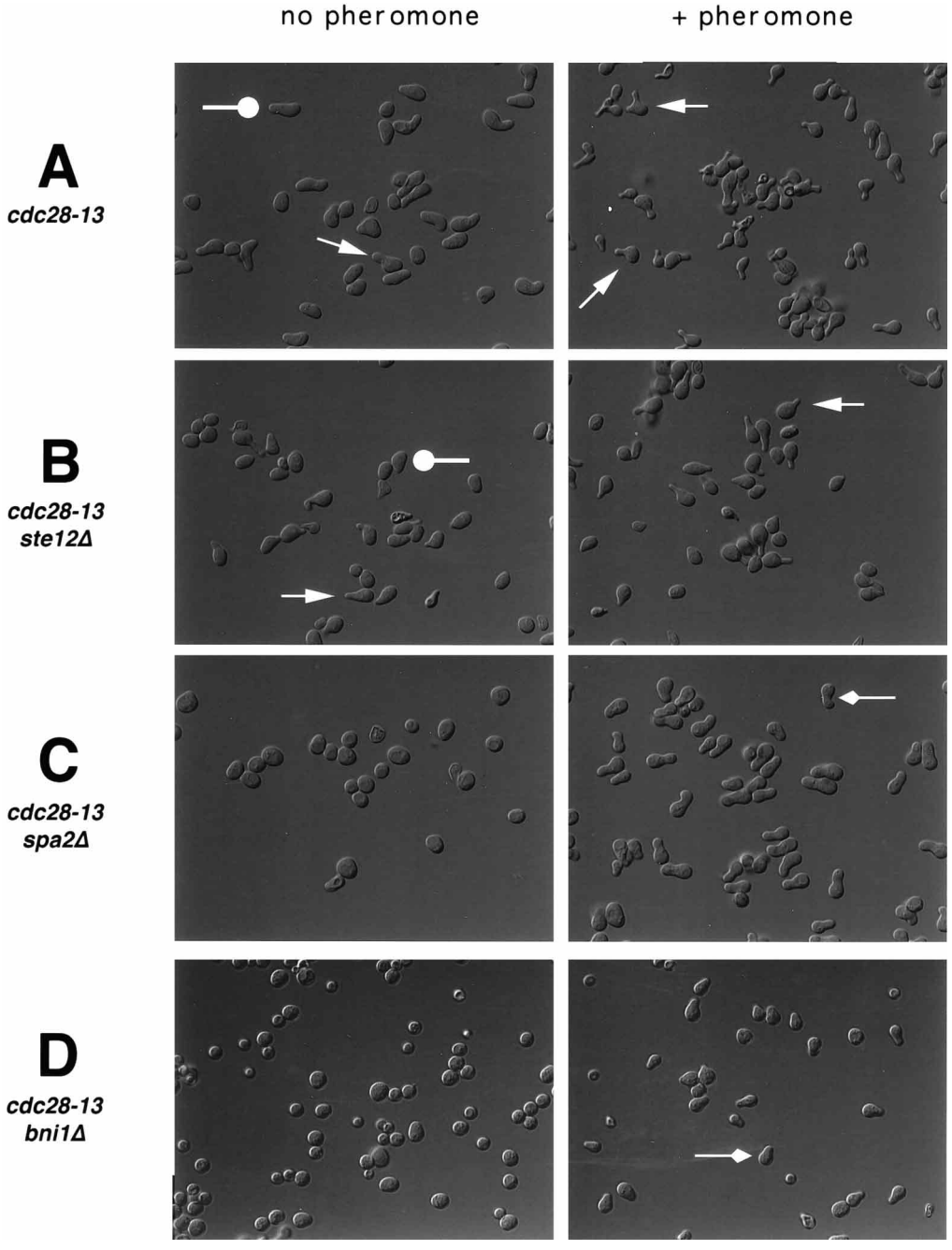

FIG. 2. Pheromone-induced morphogenesis of *cdc28-13* cells. Cultures of *cdc28-13* (13Dau), *cdc28-13 ste12*Δ (BB106), *cdc28-13 spa2*Δ (BB113), and *cdc28-13 bni1*Δ (BB126) strains were arrested in G_1 at 37°C for 2 h and treated with mating pheromone (50 nM α-factor). After 2 h in the presence (+ pheromone) or absence (no pheromone) of α-factor, morphological changes were viewed microscopically. Circle-headed arrows indicate representative cells with abnormal morphology that is characteristic of *cdc28-13* arrested cells. These are not mating projections. Arrows indicate cells representative of normal projections; diamond-headed arrows indicate representative cells with the peanut morphology typical of *spa2*Δ and *bni1*Δ cells. The percentages of cells in these fields with projections in the absence and presence of pheromone, respectively, are 29 and 78% (3% two projections) (A), 33 and 61% (B), 0 and 77% (C), and 0 and 63% (D).

to inhibit protein synthesis 15 min prior to the addition of pheromone. In the absence of protein synthesis, cells failed to form mating projections and failed to stimulate Mpk1 enzyme activity (Fig. 4B). Even without pheromone stimulation, cycloheximide caused a marked accumulation of pY-Mpk1, showing that this inactive species accumulates when the protein synthesis is blocked (Fig. 4A). These and the above results support the model that synthesis of one or more Ste12-dependent proteins is required for full activation of Mpk1 by mating pheromone. This requirement suggests that some consequence of mating differentiation may be the signal leading to Mpk1 activation.

The cell integrity kinase cascade is required for pheromone-induced MPK1 activation. The Pkc1, Bck1, and Mkk1/2 protein kinases form the cascade that leads to activation of Mpk1 in response to heat shock and cell proliferation (28, 36). We

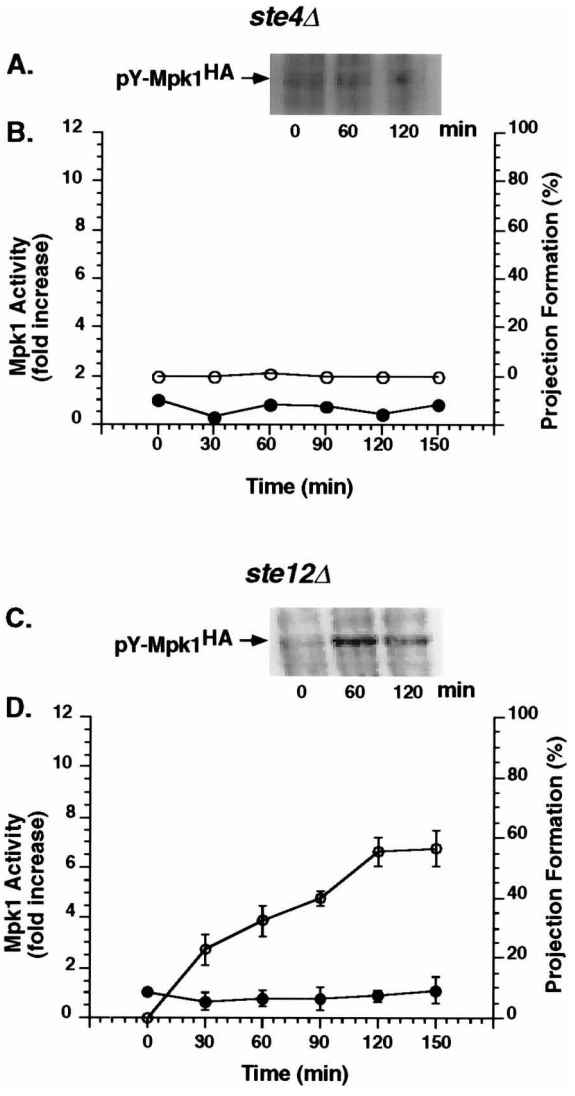

FIG. 3. Pheromone-induced activation of Mpk1 requires Ste4-Gβ and Ste12. Cultures of a *cdc28-13 ste4*Δ strain (BB131) (A and B) and a *cdc28-13 ste12*Δ strain (BB106) (C and D) were arrested in G_1 at 37°C and treated with mating pheromone (50 nM α-factor, $t = 0$). (A and C) Western blots showing tyrosine-phosphorylated Mpk1 (pY-$Mpk1^{HA}$) at indicated times. (B and D) Fold increase in Mpk1 activity (solid circles) and percentage of cells in the culture with mating projections (open circles) at indicated times as defined for Fig. 1. Data shown in panels B and D are averages of two and three experiments, respectively. Bars show the deviation in the measurements. Panels A and C are representative examples of these trials.

tested yeast strains carrying disruptions of these enzymes to determine if this same cascade also mediates Mpk1 activation in response to pheromone. Each mutant strain also had a temperature-sensitive *cdc28* allele that allowed us to arrest cells in G_1 and measure the pheromone-dependent activation Mpk1 separately from other stimuli of the cell integrity pathway as before. To protect the mutant strains from lysis at this elevated temperature, all cultures were in medium containing 100 mM sorbitol. This amount of sorbitol in combination with overexpressed Mpk1 prevents lysis (30, 37). Further, we have found that this concentration does not inhibit Mpk1 activity.

A *cdc28-4 pkc1*^{ts} double-mutant strain (TME-3/28) was used to test whether pheromone stimulation of Mpk1 activity is dependent on the input kinase of the cell integrity pathway.

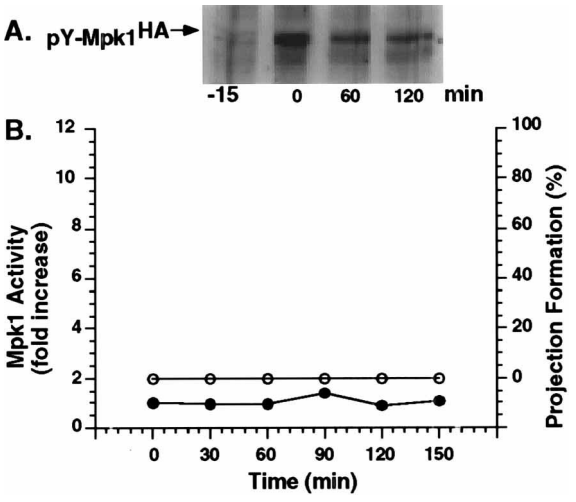

FIG. 4. Pheromone-induced activation of Mpk1 requires protein synthesis. A culture of a *cdc28-13* strain (13Dau) was arrested in G_1 at 37°C and treated with cycloheximide 15 min before ($t = -15$) addition of mating pheromone (50 nM α-factor, $t = 0$). (A) Western blot showing tyrosine-phosphorylated Mpk1 (pY-$Mpk1^{HA}$) at indicated times. (B) Fold increase in Mpk1 activity (solid circles) and percentage of cells in the culture with mating projections (open circles) at indicated times as defined for Fig. 1. Data in panel B are the averages of two experiments. The standard deviations were less than the size of the symbols and are not shown. Panel A is representative of the trials.

Pheromone response failed to stimulate tyrosine phosphorylation and activation of Mpk1 in the absence of a functional Pkc1 (Fig. 5). A *cdc28-13 bck1*Δ double-mutant strain (BB108) and a *cdc28-13 mkk1*Δ *mkk2*Δ triple-mutant strain (BB121) were analyzed to test if the known enzymes that comprise one branch of the Pkc1-dependent pathway are also required for Mpk1 activation in response to pheromone. Cells deficient in Mkk1 and Mkk2 did not stimulate tyrosine phosphorylation or

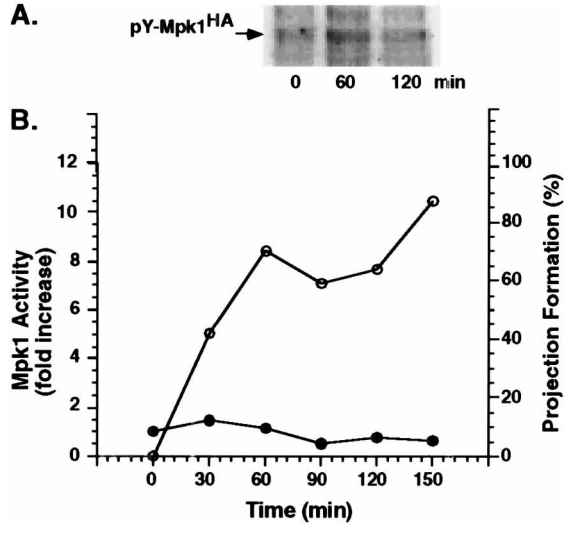

FIG. 5. Pkc1 mediates pheromone-induced activation of Mpk1. A culture of a *cdc28-4 pkc1*^{ts} strain (TME-3/28) in 100 mM sorbitol for osmotic support was arrested in G_1 at 37°C and treated with mating pheromone (50 nM α-factor, $t = 0$). (A) Western blot showing tyrosine-phosphorylated Mpk1 (pY-$Mpk1^{HA}$) at indicated times. (B) Fold increase in Mpk1 activity (solid circles) and percentage of cells in the culture with mating projections (open circles) at indicated times as defined for Fig. 1. Data in panel B are averages of three experiments. The standard deviations were less than the size of the symbols and are not shown. Panel A is a representative example of the trials.

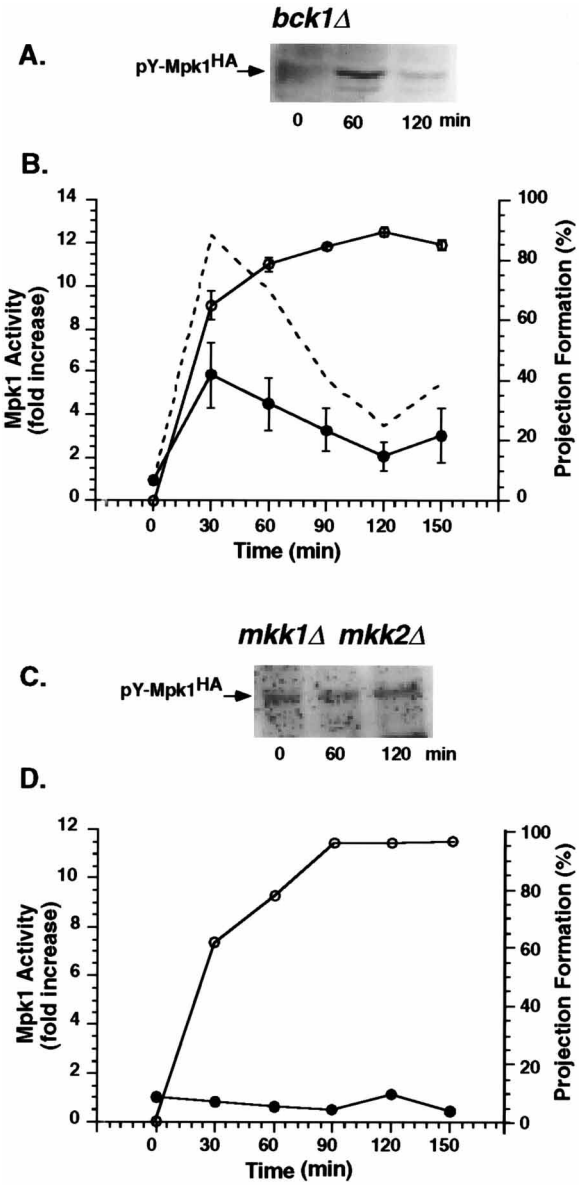

FIG. 6. Mkk1 and Mkk2, but not Bck1, are strictly required for pheromone-induced activation of Mpk1. Cultures of a *cdc28-13 bck1*Δ strain (BB108) (A and B) and a *cdc28-13 mkk1*Δ *mkk2*Δ strain (BB121) (C and D) in 100 mM sorbitol for osmotic support were arrested in G_1 at 37°C and treated with mating pheromone (50 nM α-factor, $t = 0$). (A and C) Western blots showing tyrosine-phosphorylated Mpk1 (pY-Mpk1^{HA}) at indicated times. (B and D) Fold increase in Mpk1 activity (solid circles) and percentage of cells in the culture with mating projections (open circles) at indicated times as defined for Fig. 1. Dashed line in panel B shows the pheromone-induced activation profile of Mpk1 from a parallel experiment with the *cdc28-13* strain (13Dau) for reference. Data displayed in panel B are averages of three trials. Bars show the deviation in the measurements. Data in panel D are from one trial. Panels A and C are representative examples of these trials.

activation of Mpk1 during pheromone response (Fig. 6C and D). Thus, for pheromone as for other known stimuli of the cell integrity pathway, Mkk1 and Mkk2 are presumed to be the enzymes that directly phosphorylate and activate Mpk1. Our finding that cells deficient in Bck1 still partially activated Mpk1 in response to mating pheromone was a surprise because Bck1 is the only known activator of Mkk1 and Mkk2 (Fig. 6A and B). This Bck1-independent contribution to Mpk1 activation suggests that some as yet unidentified component functionally overlaps with Bck1. This postulated component either is not expressed in some strain backgrounds or comes into play only under pheromone-induced conditions because Bck1 is absolutely required for other stimuli, such as heat shock, that activate Mpk1 (22).

Spa2 and Bni1 regulate the timing of pheromone-induced Mpk1 activation. Spa2 is a coil-coil-related protein that is known to localize at areas of polarized cell growth, such as at the tips of buds and mating projections (45). Additionally, *spa2* mutant strains form abnormal projections that are wider and more rounded than those formed by wild-type strains and show a reduced mating efficiency compared with wild-type strains (Fig. 2C) (2, 7, 16). Spa2 function is also linked with that of the cell integrity pathway because a deletion of *BCK1* is synthetically lethal with a *spa2* mutation (5). These functional relationships and the correlation between the timing of Mpk1 activation and projection formation suggested to us that Spa2 might contribute to the signal for activation of the cell integrity pathway.

To test our hypothesis, Mpk1 activation by pheromone in a *cdc28-13 spa2*Δ strain (BB113) was examined as before. Projection formation in *spa2*Δ cells was delayed ~30 min compared with that of *SPA2* cells (Fig. 7B and 1B). Mpk1 activation was delayed by the same amount of time, with its increase paralleling the appearance of peanut-shaped cells resulting from abnormal projection formation in the culture (Fig. 7B). In contrast to *SPA2* genetic background, the *spa2*Δ mutant showed no decline in Mpk1 activity for the duration of the experiment. Phosphotyrosine content of Mpk1 correlated with activity (Fig. 7A). This profile of pheromone response suggests that Spa2 contributes not only to the timing and normal morphology of mating projections but also to the timing of Mpk1 activation.

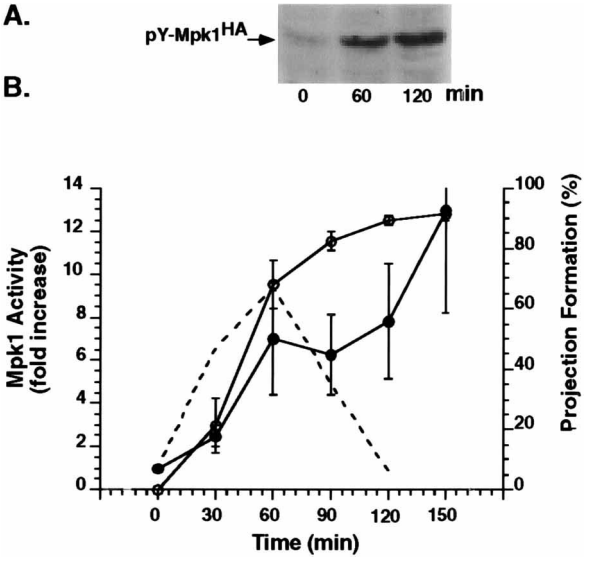

FIG. 7. Spa2 affects the timing of projection formation and pheromone-induced activation of Mpk1. A culture of a *cdc28-13 spa2*Δ strain (BB113) was arrested in G_1 at 37°C and treated with mating pheromone (50 nM α-factor, $t = 0$). (A) Western blot showing tyrosine-phosphorylated Mpk1 (pY-Mpk1^{HA}) at indicated times. (B) Fold increase in Mpk1 activity (solid circles) and percentage of cells in the culture with mating projections (open circles) at indicated times as defined for Fig. 1. The dashed line shows the pheromone-induced activation profile of Mpk1 from a parallel experiment with the *cdc28-13* strain (13Dau) for reference. Data in panel B are averages of six experiments. Bars show the deviation in measurements. Panel A is a representative example of these trials.

Bni1 is a member of the formin family of proteins that localizes to the same sites as Spa2 (11, 33). Like Spa2, it has a role in septation and polar bud site selection characteristic of diploid yeast (14, 33, 50). In addition, Bni1 recently was found to interact directly with Rho1, a known activator of Pkc1 (23, 24). Because of these known similarities and relationships, we tested whether a *cdc28-13 bni1*Δ mutant strain (BB126) would show a similar alteration in pheromone-induced projection formation and Mpk1 activation. Like the *spa2*Δ mutant, the *bni1*Δ mutant made abnormal projections which were much more rounded and wider than those in wild-type cells (Fig. 2D). However, the projections arose at an even more delayed time than in the *spa2*Δ strain (Fig. 8B and 7B). Pheromone-induced Mpk1 activity was similarly delayed (Fig. 8).

To test whether Spa2 and Bni1 have additive functions regarding their effects on the timing of projection formation and Mpk1 activation, we constructed a *cdc28-13 bni1*Δ *spa2*Δ mutant strain (BB127). The *bni1*Δ *spa2*Δ double mutant still formed projections and showed an increase in Mpk1 activity (Fig. 8D). The timing of these responses with the *bni1*Δ *spa2*Δ double mutant was essentially the same as for the *bni1*Δ single mutant (Fig. 8D). The nonadditive phenotype of the double mutant is consistent with a model in which Spa2 and Bni1 function in the same genetic pathway rather than in separate pathways that impinge on the same function.

DISCUSSION

Pheromone-induced differentiation of haploid yeast into a mating-competent form involves the elaboration of mating projections that are oriented toward their mating partners. We previously reported that cells lacking a functional cell integrity pathway lyse when elaborating mating projections and that pheromone stimulates Mpk1 activity (9). Therefore, pheromone-induced activation of this second pathway is important for cells to remain viable during mating differentiation. In this study, we examined the mechanism by which a single stimulus, pheromone, activates two separate MAPK pathways. We found that activation of Mpk1 requires Ste12-dependent transcription and synthesis of one or more proteins. The dependence on protein synthesis distinguishes the pheromone-dependent activation of Mpk1 from that of the mating pathway MAPKs which are phosphorylated and activated even in the presence of cycloheximide (15). It is noteworthy that Mpk1 activation does not generally depend on protein synthesis because heat shock stimulation of Mpk1 activity occurs in the presence of cycloheximide (22). These results support the view that activation of the cell integrity pathway MAPK, Mpk1, occurs in response to the output of the mating pathway rather than through a more direct signaling mechanism.

Other evidence in this paper shows that coordination of Mpk1 activation during pheromone response involves some aspect of mating projection formation. The kinetics of pheromone-induced Mpk1 activation is bimodal. The first rise in Mpk1 activity parallels the appearance of a single projection on cells in the culture. Upon prolonged exposure to mating pheromone, some cells elaborate a second mating projection (Fig. 2A). The second rise in Mpk1 activity parallels the appearance of these second projections. Moreover, mutations that delay the timing of projection formation delay Mpk1 activation. Mutant strains that have a deficiency in Spa2 or Bni1 are delayed in projection formation and Mpk1 activation compared with wild-type cells by 30 or 60 min, respectively. This correlation suggests that the process of projection formation may provide at least part of the signal that leads to activation of Mpk1. However, the stimulus associated with projection formation cannot be sufficient for the Mpk1 activation. At the nonpermissive temperature, *cdc28-13 ste12*Δ mutants still respond to pheromone by producing mating projections and activating Fus3, yet they fail to show an increase in Mpk1 activity. Therefore, we propose that two responses to pheromone induction, synthesis of a Ste12-dependent protein(s) and

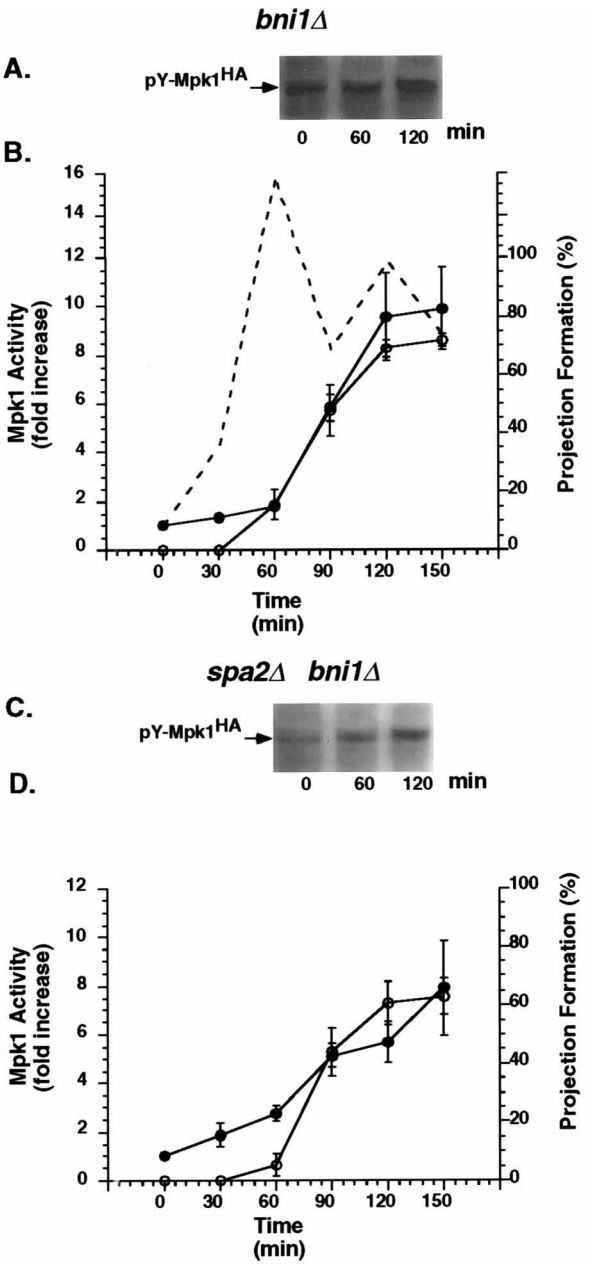

FIG. 8. Bni1 affects the timing of projection formation and pheromone-induced activation of Mpk1. Cultures of a *cdc28-13 bni1*Δ strain (BB126) (A and B) and a *cdc28-13 spa2*Δ *bni1*Δ strain (BB127) (C and D) were arrested in G_1 at 37°C and treated with mating pheromone (50 nM α-factor, $t = 0$). (A and C) Western blots showing tyrosine-phosphorylated Mpk1 (pY-Mpk1^{HA}) at indicated times. (B and D) Fold increase in Mpk1 activity (solid circles) and percentage of cells in the culture with mating projections (open circles) at indicated times as defined for Fig. 1. Dashed lines show the pheromone-induced activation profile of Mpk1 from parallel experiments with a *cdc28-13* strain (13Dau) for reference. Data displayed in panels B and D are averages of three experiments. Bars show the deviation in the measurements. Panels A and C are representative examples of the trials.

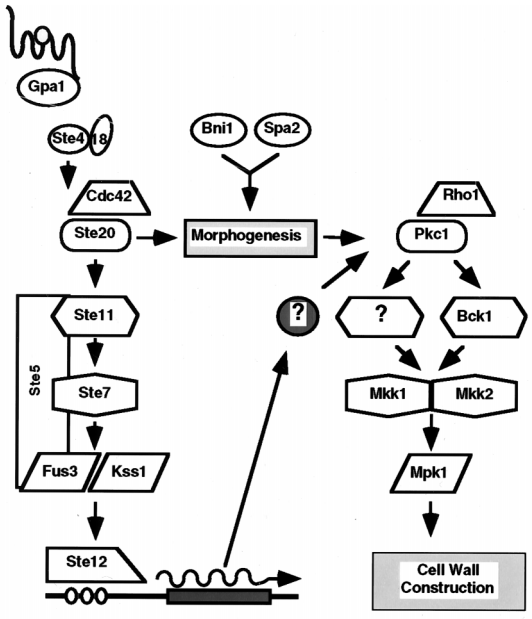

FIG. 9. Model for pheromone-induced activation of Mpk1. Mating pheromone stimulates the mating response signal transduction pathway (left) that mediates the production of mating-specific proteins and morphogenesis leading to mating projection formation. Spa2 and Bni1 also regulate morphogenesis in that they affect the timing and quality of mating projection formation. Both Ste12-dependent gene expression and morphogenesis are required for the signal that activates the cell integrity pathway (right). This signal stimulates Pkc1 which mediates Bck1-dependent and -independent mechanisms for activation of Mkk1 and Mkk2, the direct activators of Mpk1.

morphogenesis of mating projections, serve as second messengers to coordinate Mpk1 activation during mating differentiation (Fig. 9).

The pheromone-induced messengers appear to act at or before the level of Pkc1. Evidence for where the signal intersects the cell integrity pathway came from the analysis of mutants with deficiencies or defects in the enzymes of this pathway. In the absence of a functional Pkc1, cells respond to pheromone and form mating projections but fail to activate Mpk1. Mkk1 and Mkk2 also are strictly required for the activation and therefore are presumably the enzymes that directly catalyze the phosphorylations required for Mpk1 catalytic competence. Interestingly, there is only a partial requirement for Bck1, which is the only known activator of Mkk1 and Mkk2. Therefore, an alternate mechanism for the Pkc1-dependent activation of Mkk1/Mkk2, which involves an as yet unidentified component or components, is available in the BF264-15D strain background (Fig. 9). Mpk1 activation by heat shock has been reported to be completely dependent on Bck1 (22). Because we do not observe heat shock activation of Mpk1 in the BF264-15D strain background, the experiment cannot be done to test whether the alternative mechanism also acts during heat shock activation of the pathway. However, the postulated component cannot generally compensate for a deficiency in Bck1 because we still find that a *spa2*Δ *bck1*Δ double mutant is inviable in the BF264-15D strain background. Therefore, it is possible that the alternate mechanism is specific for mating pheromone induction of Mpk1 activity.

Spa2 and Bni1 also have a role in coordinating the activities of the mating and cell integrity pathways (Fig. 9). These proteins are localized to sites of polarized cell growth as determined by indirect immunofluorescence, showing up as a sharp crescent of protein at the incipient bud site, the bud tip, or the projection tip (33, 45, 46). Mutant cells lacking Spa2 or Bni1 form wider and more rounded projections compared with those in wild-type cells (Fig. 2C and D) (16). As noted above, these aberrant projections appear with a delayed timing in the mutant cells compared with wild-type cells, and this delay is associated with the same delay in Mpk1 activation. Interestingly, Spa2 and, presumably, Bni1 are not universally required for activation of the cell integrity pathway. A *spa2* deletion was found not to affect the timing or extent of Mpk1 activation by heat shock (22a). Therefore, the different stimuli for the cell integrity pathway may utilize different mechanisms for activation of the MAPK cascade.

Our model for how pheromone induction causes activation of Mpk1 differs from the one proposed by Zarzov et al. (51). We propose that two cellular responses to pheromone provide a link between the pathways, while Zarzov et al. propose that Ste20 is the link (51). The latter model derives in part from their conclusion that pheromone induction of Mpk1 activity does not require the Ste12 transcription factor. They came to this incorrect conclusion because their studies relied on phosphotyrosine content as the sole criterion for assessing Mpk1 activity in *ste12*Δ mutant cells (see our data in Fig. 3C and D). Also, they did not uncover the fact that protein synthesis is required for pheromone-induced activation of Mpk1. This condition is difficult to rationalize with their model because Ste20 activation occurs independently of protein synthesis. Another difference between the two models stems from the finding of Zarzov et al. that activation of Mpk1 strictly requires Bck1, whereas we find that there is only a partial requirement for this enzyme (51). As discussed above, it is possible that the alternative pathway that we propose for the activation of Mkk1 and Mkk2 operates in some strain backgrounds but not in others.

Our model still gives Ste20 a pivotal role in the pheromone-induced activation of the cell integrity pathway, but this is because Ste20 has dual roles during mating differentiation. One is in promoting morphogenesis, and the other is in the activation of the MAPK cascade, whose output is essential for activity of the Ste12 transcription factor (26, 38, 40). Therefore, its absence would block the two responses that we show are required for pheromone induction of Mpk1 activity.

The coordination of the mating and cell integrity pathways still poses difficult questions. For example, we do not know the identity or function of the Ste12-dependent protein or proteins that are required for the activation. It is also unclear how morphogenesis generates the signal used to stimulate the cell integrity pathway. Stretching of the plasma membrane occurs with each of the conditions known to stimulate Mpk1 activation, including (i) polarized growth associated with proliferation and projection formation and (ii) distortions that occur upon hypotonic or heat shock. Therefore, a stretch-activated membrane channel could trigger activation of the cell integrity pathway (22, 31, 51). Our findings that implicate Bni1 and Spa2 in the timing of projection formation and Mpk1 activation open the possibility that the molecular machinery used to select sites of projection formation is important for its activation during pheromone response. It appears that Bem1, Cdc24, Far1, Bni1, and Spa2 all play a role in projection formation (2, 16, 47). The mechanism whereby these proteins interact with each other, the mating pathway, and the cell integrity pathway may provide an important link between these pathways.

ACKNOWLEDGMENTS

We thank Y. Kamada and D. Levin for sharing unpublished observations and for helpful discussions. We thank S. Reed, D. Levin, S. Fields, M. Snyder, K. Irie, and J. Pringle for sharing plasmids and strains used in this study.

This research was supported by Public Health grant GM-39852 from the National Institutes of Health.

REFERENCES

1. **Brill, J. A., E. A. Elion, and G. R. Fink.** 1994. A role for autophosphorylation revealed by activated alleles of FUS3, the yeast MAP kinase homolog. Mol. Biol. Cell **5:**297–312.
2. **Chenevert, J., N. Valtz, and I. Herskowitz.** 1994. Identification of genes required for normal pheromone-induced cell polarization in *Saccharomyces cerevisiae*. Genetics **136:**1287–1296.
3. **Choi, K.-Y., B. Satterberg, D. M. Lyons, and E. A. Elion.** 1994. Ste5 tethers multiple protein kinases in the MAP kinase cascade required for mating in *S. cerevisiae*. Cell **78:**499–512.
4. **Christianson, T. W., R. S. Sikorski, M. Dante, J. H. Shero, and P. Hieter.** 1992. Multifunctional yeast high-copy-number shuttle vectors. Gene **110:** 119–122.
5. **Costigan, C., S. Gehrung, and M. Snyder.** 1992. A synthetic lethal screen identifies SLK1, a novel protein kinase homolog implicated in yeast cell morphogenesis and cell growth. Mol. Cell. Biol. **12:**1162–1178.
6. **Cross, R., L. H. Hartwell, C. Jackson, and J. B. Konopka.** 1988. Conjugation in *Saccharomyces cerevisiae*. Annu. Rev. Cell Biol. **4:**429–457.
7. **Dorer, R., P. M. Pryciak, and L. H. Hartwell.** 1995. *Saccharomyces cerevisiae* cells execute a default pathway to select a mate in the absence of pheromone gradients. J. Cell Biol. **131:**845–861.
8. **Elion, E. A., J. A. Brill, and G. R. Fink.** 1991. FUS3 represses CLN1 and CLN2 and in concert with KSS1 promotes signal transduction. Proc. Natl. Acad. Sci. USA **88:**9392–9396.
9. **Errede, B., R. M. Cade, B. M. Yashar, Y. Kamada, D. E. Levin, K. Irie, and K. Matsumoto.** 1995. Dynamics and organization of MAP kinase signal pathways. Mol. Reprod. Dev. **42:**477–485.
10. **Errede, B., A. Gartner, Z. Zhou, K. Nasmyth, and G. Ammerer.** 1993. MAP kinase-related FUS3 from S. cerevisiae is activated by STE7 in vitro. Nature **362:**261–264.
11. **Evangelista, M., K. Blundell, M. S. Longtine, C. J. Chow, N. Adames, J. R. Pringle, M. Peter, and C. Boone.** 1997. Bni1p, a yeast formin linking Cdc42p and the actin cytoskeleton during polarized morphogenesis. Science **276:** 118–122.
12. **Fields, S., D. T. Chaleff, and G. F. Sprague, Jr.** 1988. Yeast *STE7*, *STE11*, and *STE12* genes are required for expression of cell-type-specific genes. Mol. Cell. Biol. **8:**551–556.
13. **Fields, S., and I. Herskowitz.** 1987. Regulation by the yeast mating-type locus of *STE12*, a gene required for cell-type-specific expression. Mol. Cell. Biol. **7:**3818–3821.
14. **Flescher, E. G., K. Madden, and M. Snyder.** 1993. Components required for cytokinesis are important for bud site selection in yeast. J. Cell Biol. **122:** 373–386.
15. **Gartner, A., K. Nasmyth, and G. Ammerer.** 1992. Signal transduction in *Saccharomyces cerevisiae* requires tyrosine and threonine phosphorylation of FUS3 and KSS1. Genes Dev. **6:**1280–1292.
16. **Gehrung, S., and M. Snyder.** 1990. The SPA2 gene of *Saccharomyces cerevisiae* is important for pheromone-induced morphogenesis and efficient mating. J. Cell Biol. **111:**1451–1464.
17. **Gietz, R. D., and A. Sugino.** 1988. New yeast-*Escherichia coli* shuttle vectors constructed with *in vitro* mutagenized yeast genes lacking six-base pair restriction sites. Gene **74:**527–534.
18. **Hartwell, L. H.** 1980. Mutants of *Saccharomyces cerevisiae* unresponsive to cell division control by polypeptide mating hormone. J. Cell Biol. **85:**811–822.
19. **Herskowitz, I.** 1995. MAP kinase pathways in yeast: for mating and more. Cell **80:**187–197.
20. **Irie, K., M. Takase, K. S. Lee, D. E. Levin, H. Araki, K. Matsumoto, and Y. Oshima.** 1993. *MKK1* and *MKK2*, which encode *Saccharomyces cerevisiae* mitogen-activated protein kinase-kinase homologs, function in the pathway mediated by protein kinase C. Mol. Cell. Biol. **13:**3076–3083.
21. **Ito, H., Y. Fukuda, K. Murata, and A. Kimura.** 1983. Transformation of intact yeast cells treated with alkali cations. J. Bacteriol. **153:**163–168.
22. **Kamada, Y., U. S. Jung, J. Piotrowski, and D. E. Levin.** 1995. The protein kinase C-activated MAP kinase pathway of *Saccharomyces cerevisiae* mediates a novel aspect of the heat shock response. Genes Dev. **9:**1559–1571.

22a. **Kamada, Y., and D. Levin.** Personal communication.

23. **Kamada, Y., H. Qadota, C. P. Python, Y. Anraku, Y. Ohya, and D. E. Levin.** 1996. Activation of yeast protein kinase C by Rho1 GTPase. J. Biol. Chem. **271:**9193–9196.
24. **Khono, H., T. Kazuma, A. Mino, M. Umikawa, H. Imamura, T. Fujiwara, Y. Fujita, K. Hotta, H. Qadota, T. Watanabe, Y. Ohya, and Y. Takai.** 1996. Bni1p implicated in cytoskeletal control is a putative target of Rho1p small GTP binding protein in *Saccharomyces cerevisiae*. EMBO J. **15:**6060–6068.
25. **Laemmli, U. K.** 1970. Cleavage of structural proteins during the assembly of the head of bacteriophage T4. Nature **227:**680–685.
26. **Leberer, E., D. Dignard, D. Harcus, D. Y. Thomas, and M. Whiteway.** 1992. The protein kinase homologue Ste20p is required to link the yeast pheromone response G-protein beta gamma subunits to downstream signalling components. EMBO J. **11:**4815–4824.
27. **Lee, K. S., L. K. Hines, and D. E. Levin.** 1993. A pair of functionally redundant yeast genes (*PPZ1* and *PPZ2*) encoding type 1-related protein phosphatases function within the PKC1-mediated pathway. Mol. Cell. Biol. **13:**5843–5853.
28. **Lee, K. S., K. Irie, Y. Gotoh, Y. Watanabe, H. Araki, E. Nishida, K. Matsumoto, and D. E. Levin.** 1993. A yeast mitogen-activated protein kinase homolog (Mpk1p) mediates signalling by protein kinase C. Mol. Cell. Biol. **13:**3067–3075.
29. **Lee, K. S., and D. E. Levin.** 1992. Dominant mutations in a gene encoding a putative protein kinase (*BCK1*) bypass the requirement for a *Saccharomyces cerevisiae* protein kinase C homolog. Mol. Cell. Biol. **12:**172–182.
30. **Levin, D. E., and E. Bartlett-Heubusch.** 1992. Mutants in the *S. cerevisiae* PKC1 gene display a cell cycle-specific osmotic stability defect. J. Cell Biol. **116:**1221–1229.
31. **Levin, D. E., and B. Errede.** 1995. The proliferation of MAP kinase signaling pathways in yeast. Curr. Opin. Cell Biol. **7:**197–202.
32. **Levin, D. E., F. O. Fields, R. Kunisawa, J. M. Bishop, and J. Thorner.** 1990. A candidate protein kinase C gene, *PKC1*, is required for the *S. cerevisiae* cell cycle. Cell **62:**213–224.
33. **Longtine, M. S., D. J. DeMarini, M. L. Valencik, O. S. Al-Awar, H. Fares, C. De Virgilio, and J. R. Pringle.** 1996. The septins: roles in cytokinesis and other processes. Curr. Opin. Cell Biol. **8:**106–119.
34. **Marcus, S., A. Polverino, M. Barr, and M. Wigler.** 1994. Complexes between STE5 and components of the pheromone-responsive mitogen-activated protein kinase module. Proc. Natl. Acad. Sci. USA **91:**7762–7766.
35. **Marini, N. J., E. Meldrum, B. Buehrer, A. V. Hubberstey, D. Stone, A. Traynor-Kaplan, and S. I. Reed.** 1996. A pathway in the yeast cell division cycle linking protein kinase C (Pkc1) to activation of Cdc28 at START. EMBO J. **15:**3040–3052.
36. **Mazzone, C., P. Zarzov, A. Rambourg, and C. Mann.** 1993. The SLT2 (MPK1) MAP kinase homolog is involved in polarized cell growth in *Saccharomyces cerevisiae*. J. Cell Biol. **123:**1821–1833.
37. **Paravicini, G., M. Cooper, L. Friedli, D. J. Smith, J.-L. Carpentier, L. S. Klig, and M. A. Payton.** 1992. The osmotic integrity of yeast cell requires a functional *PKC1* gene product. Mol. Cell. Biol. **12:**4896–4905.
38. **Peter, M., A. M. Neiman, H.-O. Park, M. van Lohuizen, and I. Herskowitz.** 1996. Functional analysis of the interaction between the small GTP binding protein Cdc42 and the Ste20 protein kinase in yeast. EMBO J. **15:**7046–7059.
39. **Printen, J. A., and G. F. Sprague, Jr.** 1994. Protein-protein interactions in the yeast pheromone response pathway: Ste5p interacts with all members of the MAP kinase cascade. Genetics **138:**609–619.
40. **Ramer, S. W., and R. W. Davis.** 1993. A dominant truncation allele identifies a gene, STE20, that encodes a putative protein kinase necessary for mating in *Saccharomyces cerevisiae*. Proc. Natl. Acad. Sci. USA **90:**452–456.
41. **Reed, S. I., J. A. Hadwiger, and A. Lorincz.** 1985. Protein kinase activity associated with the product of the yeast cell division cycle gene CDC28. Proc. Natl. Acad. Sci. USA **82:**4055–4059.
42. **Rothstein, R. J.** 1983. One-step gene disruption in yeast. Methods Enzymol. **101:**202–211.
43. **Segall, J. E.** 1993. Polarization of yeast cells in spatial gradients of alpha mating factor. Proc. Natl. Acad. Sci. USA **90:**8332–8336.
44. **Sherman, F., G. R. Fink, and J. B. Hicks.** 1979. Methods in yeast genetics. Cold Spring Harbor Laboratory, Cold Spring Harbor, N.Y.
45. **Snyder, M.** 1989. The SPA2 protein of yeast localizes to sites of cell growth. J. Cell Biol. **108:**1419–1429.
46. **Snyder, M., S. Gehrung, and B. Page.** 1991. Studies concerning the temporal and genetic control of cell polarity in *Saccharomyces cerevisiae*. J. Cell Biol. **114:**515–532.
47. **Valtz, N., M. Peter, and I. Herskowitz.** 1995. FAR1 is required for oriented polarization of yeast cells in response to mating pheromones. J. Cell Biol. **131:**863–873.
48. **Wilson, I. A., H. L. Niman, R. A. Houghten, A. R. Cherenson, M. L. Connolly, and R. A. Lerner.** 1984. The structure of an antigenic determinant in a protein. Cell **37:**767–778.
49. **Yashar, B., K. Irie, J. A. Printen, B. J. Stevenson, G. J. Sprague, K. Matsumoto, and B. Errede.** 1995. Yeast MEK-dependent signal transduction: response thresholds and parameters affecting fidelity. Mol. Cell. Biol. **15:**6545–6553.
50. **Zahner, J. E., H. A. Harkins, and J. R. Pringle.** 1996. Genetic analysis of the bipolar pattern of bud site selection in the yeast *Saccharomyces cerevisiae*. Mol. Cell. Biol. **16:**1857–1870.
51. **Zarzov, P., C. Mazzoni, and C. Mann.** 1996. The SLT2 (MPK1) MAP kinase is activated during periods of polarized cell growth in yeast. EMBO J. **15:** 83–91.
52. **Zhou, Z., A. Gartner, R. Cade, G. Ammerer, and B. Errede.** 1993. Pheromone-induced signal transduction in *Saccharomyces cerevisiae* requires the sequential function of three protein kinases. Mol. Cell. Biol. **13:**2069–2080.